
Grounding Multimodal Large Language Models in Actions

Andrew Szot^{1,2} Bogdan Mazoure¹ Harsh Agrawal¹ Devon Hjelm^{1,3}
Zsolt Kira² Alexander Toshev¹
¹ Apple, ² Georgia Tech, ³ Mila
a.szot@apple.com, toshev@apple.com

Abstract

Multimodal Large Language Models (MLLMs) have demonstrated a wide range of capabilities across many domains, including Embodied AI. In this work, we study how to best ground a MLLM into different embodiments and their associated action spaces, with the goal of leveraging the multimodal world knowledge of the MLLM. We first generalize a number of methods through a unified architecture and the lens of action space adaptors. For continuous actions, we show that a learned tokenization allows for sufficient modeling precision, yielding the best performance on downstream tasks. For discrete actions, we demonstrate that semantically aligning these actions with the native output token space of the MLLM leads to the strongest performance. We arrive at these lessons via a thorough study of seven action space adapters on five different environments, encompassing over 114 embodied tasks.

1 Introduction

Multimodal Large Language Models (MLLMs), defined as Large Foundation Models that take as input text and images and generate text, have recently seen rapid progress and impressive performance [1–13]. These models are important as they solve a large range of useful yet difficult natural language and image tasks, such as describing images, answering visual and textual questions, reasoning, and learning from a small number of examples. They have only recently improved to the point of being usable enough for general deployment with human non-experts [14–16].

While MLLMs are capable of describing real-world embodied concepts, their capabilities in embodied tasks are limited to using text for actions through generating code [17, 18], representing actions as text [19], or extracting actions from internal representations [20, 21]. *Grounding* [22] MLLMs to generate actions extends their capabilities to embodied tasks, such as robot manipulation and navigation, and is of tremendous value for practical problems, potentially overcoming the high cost of training tabula rasa. Extending MLLMs to multimodal image generation enables object detection and segmentation, and image and video generation [3, 23–27]. In embodied settings, grounding MLLMs via predicting agent affordances and generating actions yields effective policies capable of generalizing to new tasks [19, 21, 28, 29].

A key and open challenge in grounding MLLMs, which limits their capabilities in embodied tasks, is the gap between the native output space, natural language, and the action space of embodied agents. This problem is particularly acute in continuous action spaces, where low-level controllers may require a high degree of precision. Across the literature, a number of architectures and ways of handling action spaces have been proposed, but there has not been a systematic study of these designs. Our contributions generalize prior attempts to adapt MLLMs to generate actions through an empirical study on which principles and strategies are necessary to effectively close the gap between the action spaces of MLLMs and embodied agents. We study various grounding re-parameterization

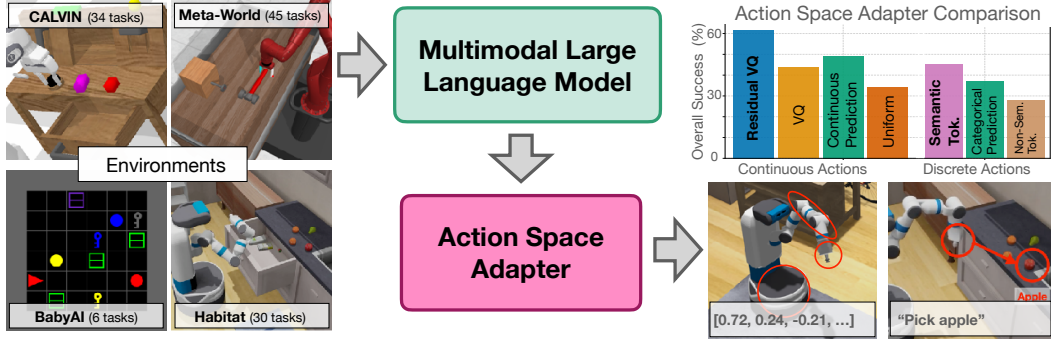


Figure 1: We empirically analyze how to ground MLLMs in actions across 114 tasks in continuous and discrete action spaces. In each environment, we train a multi-task policy with different Action Space Adapters (ASAs) to re-parameterize the MLLM to output actions. For continuous actions, learning a tokenization with several tokens per-action performs best (Residual VQ). For discrete actions, mapping actions to semantically related language tokens performs best (Semantic Tokenization).

strategies, which we refer to as Action Space Adapter (ASA), across a range of embodiments, action spaces, and environments. In particular, we explore the following types of ASAs: (1) ASAs that directly generate actions from a new prediction policy using the MLLM hidden representations as input; (2) ASAs that reuse the native token space of the MLLM to encode actions; (3) and ASAs that introduce a new token space to encode the actions of the agent while adapting the MLLMs to predict these new tokens.

Further, we empirically identify important principles for designing ASAs. For continuous action spaces, learned tokenization with several vocabularies that residually model continuous actions gives the right modeling precision while using vocabularies of manageable sizes and, as a result, yields the best performance across all continuous control environments. This learned tokenization outperforms direct action prediction, indicating this approach allows the model to effectively learn a multimodal distribution over action spaces. In addition, the above tokenization strategy boosts performance when the policy is a MLLM, compared to other standard non-LLM-based policies, indicating that it manages to better tap into the knowledge of the model.

For discrete action spaces, we study ASAs that better align the embodied actions with the output space of the MLLM. We demonstrate that a semantic alignment between these – mapping discrete actions to semantically related tokens in the MLLM vocabulary – yields the best strategy compared to other adapters that either reuse or define a new vocabulary. The superiority of this strategy is evident in performance on environments with discrete action spaces and also in RL sample efficiency.

Finally, the above principles are thoroughly validated across five embodied AI environments, three of which are robotic continuous control and two with discrete actions as illustrated in Figure 1. Altogether, we consider 114 language specified tasks. In the continuous case, the best tokenization achieves 72% on CALVIN [30], up from 68% for direct action regression and 28% for uniform action tokenization; and 84% on Meta-World [31], up from 61% for direct action regression and 75% for uniform tokenization. Similarly, in the case of discrete actions, the proposed semantically aligned action tokens yield 51% on LangR [21], up from 42% for direct action prediction.

2 Related Work

Prior works propose different Action Space Adapters (ASAs) to adapt MLLMs into policies. Some works use LLMs or MLLMs as zero-shot policies by prompting them to output text or code that can be executed as actions [18, 32–38]. The ASA in this case is a given executor or low-level controller that takes text as input and outputs actions in the environment. Other works investigate adapting MLLMs for actions, but focus on a single ASA and environment. For example, RT-2 [19] uniformly discretizes continuous actions and predicts tokens corresponding to each of the action dimensions. RoboFlamingo [20], Lamo [39], and LLaRP [21] use an MLP to predict an environment action from an LLM hidden state. GFlan [40] treats discrete actions as text and ranks actions by the LLM log

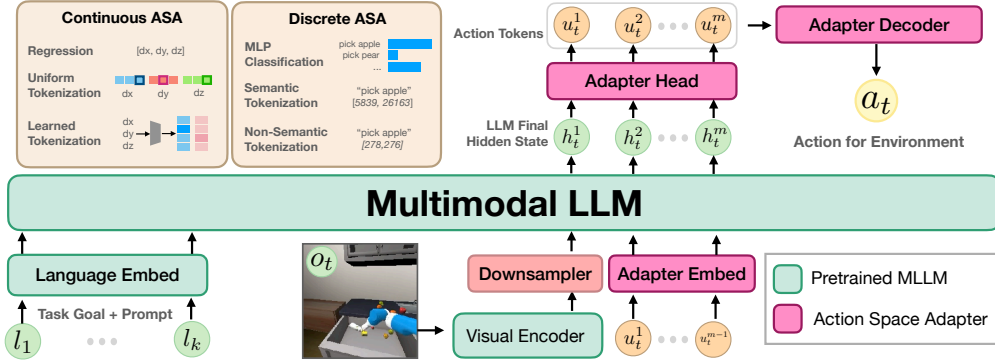


Figure 2: Generic architecture studied here for adapting MLLMs for action-specific decision making. The MLLM takes the embedding of the task instruction, prompt, and visual tokens as input. The MLLM then autoregressively predicts a sequence of m action tokens. These action tokens are then decoded into an environment-specific action.

probability to form a distribution over actions. At a high level, our work is distinct in that we study a variety of methods across multiple environments for learning ASAs. We focus on tasks with low zero-shot VLM performance, such as low-level control or long-horizon planning tasks. We summarize the differences between our investigation and prior work adapting VLMs for action in Appendix A.

Investigating action representations in embodied settings is not new. Some works learn representations of actions to help generalization to new actions or operating in large action spaces [41, 42] in the context of Reinforcement Learning (RL). Our study proposes ASAs for tokenizing continuous actions, and other works use different types of discretization or tokenization strategies on continuous action spaces. [43, 44] use k-means to discretize continuous actions to help learn from multimodal behavior datasets, such as from play data or data from different experts. VQ-BeT [45] finds learning a residual VQA (RVQ) codebook for continuous actions works best but does not apply this idea to MLLMs.

More broadly, prior works have adapted MLLMs for modalities other than actions, such as object bounding boxes and image generation, both being continuous in nature while the latter of high dimension. For example, [27, 46] train MLLMs to output spatial reference tokens to ground text responses in image regions. For image generation, [47] adapt MLLMs to generate image patches; [48, 49] tokenize images using a VQ-VAE model and adapt MLLMs to generate images by decoding these image tokens, which has inspired us to use the same learned tokenization; [50] uses an RVQ model [51] to generate images, similarly to our best performing tokenization scheme.

3 Method

In order to solve an embodied task, an agent learning in an interactive environment must select a decision from a set of valid actions. For example, an action space could be a set of keyboard presses for a video game or a real-valued vector that controls a robotic manipulator. Our work studies how to best adapt a MLLM, which is originally trained to output text tokens, to instead model actions from a given environment. We refer to the module that bridges a MLLM with a certain action space as an *Action Space Adapter* (ASA) (see Figure 2).

3.1 Problem Setting

Our analysis focuses on language-specified tasks with visual observations. Specifically, we consider a goal-specified Partially-Observable Markov Decision Process (POMDP) [52] that has an observation space \mathcal{O} , action space \mathcal{A} , and goal space \mathcal{G} . For brevity, we omit other elements of the MDP. In our setting, \mathcal{G} is a textual description of the task to solve. \mathcal{O} consists of RGB visual perception and agent proprioception. We consider a range of different action spaces \mathcal{A} that broadly fall into two categories – discrete and continuous. The primary objective is to learn a language-conditioned policy that maps observations and the instruction text to an action $\pi(a|o, g)$. As later described in Section 3.3, we

learn this policy through supervised fine tuning from expert demonstrations or reinforcement learning that maximizes the expected discounted cumulative reward of the POMDP.

3.2 From Vision and Language to Action

The process studied here for adapting MLLMs for decision making is illustrated in Figure 2. The MLLM policy takes as input a textual instruction describing the downstream task, a sequence of past observations in the task and outputs an action in the agent’s action space. In the bottom left of Fig. 2, the task description, as well as the environment description, are first encoded to produce language embeddings. To these embeddings, the MLLM then appends a sequence of visual embeddings from the current observation o_t . Since visual embeddings can often be comprised of a large number of tokens (the popular LLaVA-1.5 model [6] has 556), we introduce a downsampling layer to enable the MLLM to attend over a longer history of observations. In practice, we take the downsampling layer to be a Perceiver model [53], a learnable transformation that reduces the number of tokens from the visual encoder before being used as input to the MLLM.

The sequence of language and visual embeddings is passed through the MLLM, whose final hidden state h_t^1 encodes the entire input. The ASA, whose trainable parameters are denoted θ , is comprised of three parts: (1) an adapter head, (2) an adapter embedding, and (3) an adapter decoder. The hidden state is first passed through the adapter head to produce action tokens $u_t^1 = A_\theta(h_t^1)$. The action tokens are then embedded using the action embedding into $E_\theta(u_t^1)$, and passed autoregressively through the MLLM to produce further hidden embeddings h_t^2, \dots, h_t^m and associated action tokens u_t^2, \dots, u_t^m , resulting in total m tokens per time step. The predicted action tokens are then decoded into the final action a_t by the adapter decoder, which produces the final action $a_t = D_\theta(u_t^1, \dots, u_t^m)$. As $a_t \in \mathcal{A}$, it is then executed in the environment to produce o_{t+1} , and the process continues.

Next, we describe possible ASA implementations for discrete and continuous action spaces.

3.2.1 Discrete Action Spaces

We define the following action spaces adapters for a discrete action space \mathcal{A} :

Categorical Prediction (Pred): Implement the action space adapter as an MLP network, which predicts the logits of a categorical distribution over environment actions from the MLLM hidden state. The adapter head is an MLP that maps the hidden state h^1 directly to an action $a \in \mathcal{A}$. This amounts to producing a single action token u^1 , which directly corresponds to the action a , with the action decoder being an identity map. Both the adapter head and token embeddings are initialized from scratch. This type of ASA is used by [21].

Semantic Language (SemLang): The action space adapter predicts natural language text that maps to a discrete action. First, each action $a \in \mathcal{A}$ is described with freeform text tokenized as (l_1, \dots, l_m) . The MLLM then autoregressively predicts a sequence of m tokens, which are then decoded by the adapter decoder to the corresponding action. For example, in an action space choosing a high-level skill a could be described as “pick apple”, which is tokenized as [5839, 26163] with the LLaMA tokenizer. The MLLM then must sequentially predict token 5839, then token 26163 to call this action. Sequences of tokens corresponding to invalid actions are either avoided entirely with the token filter described in Section 3.3 or treated as a no-op. Both the adapter head and the token embeddings are re-used to be the pretrained LLM’s language head and embedding layer, respectively, meaning no additional parameters over the pretrained MLLM are added. This type of ASA is used by [29].

Non-Semantic Language (Lang): Actions are mapped to language tokens, but instead of semantically meaningful descriptions of the actions as with SemLang, the actions are mapped to sequences of numbers. For example, “pick apple” is represented with the string “5 3”. The policy must then output the tokens corresponding to this text to call this pick action.

3.2.2 Continuous Action Space Adaptors

We define the following four ASAs for a continuous D -dimensional action space \mathcal{A} : the first ASA predicts in the original action space while the other three use tokenization. At training time, we learn a policy to predict these action tokens from the ASA. At test time, we employ an action decoder that maps these action tokens to actions in the original space \mathcal{A} .

Continuous Regression (Pred): Regress to the original continuous action from the MLLM hidden state h_t^1 . This is achieved via a single-layer MLP network, which is trained using MSE loss. This ASA is used by [20, 39].

Uniform Action Tokenization (Uniform): The simplest approach is to use uniform binning of the action space. In particular, we express each action as a sequence of D tokens by quantizing each of the D action dimensions into one out of K uniform bins:

$$\text{Uniform}(a) = (k_1 \dots k_D) \quad \text{such that} \quad a_d \in \text{bin}(k_d, d)$$

where $\text{bin}(k, d)$ denotes the k^{th} bin along the d^{th} action dimension. If m_d and M_d denote the lower and upper bounds respectively of the d^{th} action dimension, then its definition reads $\text{bin}(k, d) = [m_d + k \frac{M_d - m_d}{K}, m_d + (k + 1) \frac{M_d - m_d}{K}]$. At test time, we decode predicted action tokens to the center of the corresponding bins for each dimension. This type of ASA is used by [19].

Vector Quantized Tokenization (VQ): To adapt the tokenization to the particular action space, we propose to use learned tokenization. In particular, we express each action as a single token that corresponds to the closest action code from a learned codebook V . Using encoder network f_θ that maps actions to a latent embedding space:

$$\text{VQ}(a) = (k_1) \quad \text{where} \quad k_1 = \arg \min_k \|f_\theta(a) - v_k\|_2^2$$

where $v_k \in V$. The codebook V of size K is learned over an offline dataset \mathcal{D} of actions using a VQ-VAE [54]. We overwrite K infrequently used tokens from the LLM vocabulary to represent V . We defer the full details of this tokenization process to Appendix C.2.

Residual Vector Quantized Tokenization (RVQ): Precise control requires precise action modeling that can suffer after tokenization. To increase the precision of a learned tokenization, we further investigate the use of a sequence of several action tokens as in Uniform. Similar to VQ, these tokens are from M action codebooks $V_m, m \in \{1, \dots, M\}$. However, each codebook models the residual space obtained after modeling the action using preceding codebooks, thus each subsequent token captures increasingly finer action information:

$$\text{RVQ}(a) = (k_1, \dots, k_M) \quad \text{where} \quad k_m = \arg \min_k \left\| \left(f_\theta(a) - \sum_{i=1}^{m-1} v_{k_i}^i \right) - v_k^m \right\|_2^2$$

where $v_k^i \in V_i$ is the k^{th} code from the i^{th} codebook. Such tokenization can be learned using Residual VQ-VAE [RVQ-VAE, 50] on an offline dataset of actions. The actual number of token sequences we can represent is K^M . Hence, RVQ presents the opportunity to exponentially increase the action space quantization without having to drastically increase the size of the learned individual codebooks.

3.3 Training

We use LLaVA-1.5-7B [6] as the base MLLM. In the complex environments we consider, the zero-shot performance of MLLM is poor across all ASAs, even with detailed prompts. We therefore finetune the MLLM with interactive (i.e., action-labeled) data to make it more suited for interacting with a dynamic environment.

Supervised Fine Tuning (SFT) with Expert Demonstrations: We finetune the MLLM for interactive tasks using a dataset of expert demonstrations. Each demonstration contains (1) a language description of the task, (2) a sequence of observations, and (3) a sequence of actions that successfully solve the task. Note that in this work, we are primarily interested in learning imitation policies from offline data, which can be extended to offline reinforcement learning if per-timestep rewards are included in the dataset. Specifically, we train the MLLM with supervised learning to predict the expert actions from the observations and language description in the data. While the pre-trained LLM and the visual encoder remain frozen, we finetune the ASA, the visual downsampler, and parts of the LLM with LoRA [55]. In total, the model has $\approx 100M$ learnable LLM parameters and $\approx 40M$ learnable downsampler and ASA parameters. The learned tokenization schemes (RVQ and VQ) have an additional pre-training phase, where the VAE models are first trained on actions from the offline dataset and then frozen to prevent further updates in later stages.

Reinforcement Learning (RL) from Environment Feedback We can also optionally finetune the MLLM to optimize an environment reward using RL. However, predicting actions in the MLLM

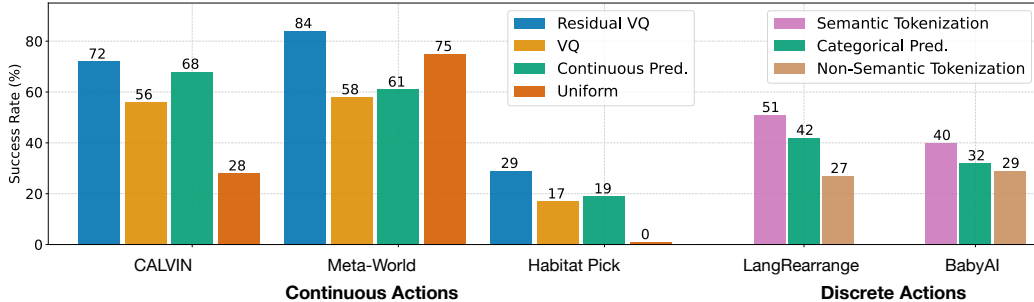


Figure 3: Comparing ASAs for continuous and discrete action spaces across 5 environments. For continuous actions, the RVQ tokenization performs best. For discrete actions, SemLang performs best. Each bar gives the average over all tasks in the environment with the full breakdown in Appendix D.

token space dramatically increases the number of possible action predictions, with many possible predictions corresponding to no valid action. For example, there are 32,000 tokens in the LLaMA text tokenizer, giving $32,000^m$ possible predictions by the model with m tokens per action. This makes exploration difficult in RL as only a small fraction of the possible actions are valid. AMLM therefore uses a *token filter* to restrict the autoregressive sampling to only be from token sequences corresponding to valid actions. The token filter is a function $M(l_t^1, \dots, l_t^{j-1})$ that produces a binary mask over all tokens to represent valid tokens for the j th decoding step.

4 Experiments

4.1 Experimental Settings

We study adapting MLLMs for action across a variety of environments with different embodiments and action spaces. All environments provide RGB visual observations and a natural language instruction specifying the goal to achieve. We provide the important environment details below and defer complete details to Appendix B.

CALVIN [30]: This manipulation benchmark tests the ability of a tabletop robot to interact with an object to complete a natural language instruction. The continuous actions specify 6DoF end-effector control and the binary gripper state. The observation is a 200×200 RGB image from a fixed-position camera. We use the $ABC \rightarrow D$ split of the benchmark with 34 tasks, and the agent is evaluated on unseen instruction phrasings and table background.

Meta-World [56]: We use the ML-45 version of this tabletop manipulation benchmark which has 45 tasks. The action space is continuous control specifying 3DoF end-effector translation and the continuous gripper state. The observations are 200×200 RGB images from a fixed camera. The agent is evaluated on unseen object and robot starting states.

Habitat Pick (HabPick) [57]: A mobile manipulation robot must pick up an object specified by name from a receptacle. The continuous actions specify the 7DoF relative joint positions of the arm, the 2D base velocity, and the gripper state. The observations are 336×336 RGB images from the robot’s egocentric head camera. The instruction specifies the name of the object type to pick up. The evaluation distribution is on unseen houses and new arrangements of objects.

BabyAI [58]: BabyAI is a grid world task where an agent navigates and interacts with objects to complete an instruction. The discrete action space consists of navigation and interaction actions. The observation is a 200×200 RGB top-down view. We use the five tasks from [40], and we report generalization to instructions rephrased with synonyms.

Language Rearrangement (LangR) [21]: A mobile manipulation robot must rearrange objects to complete instructions like “store all the fruit in the fridge”. The discrete actions are 70 high-level skills to interact with objects and navigate. The observation is a 336×336 RGB head camera. Evaluation instructions test generalization to unseen houses and 10 unseen instruction datasets measuring paraphrastic robustness and behavior generalization.

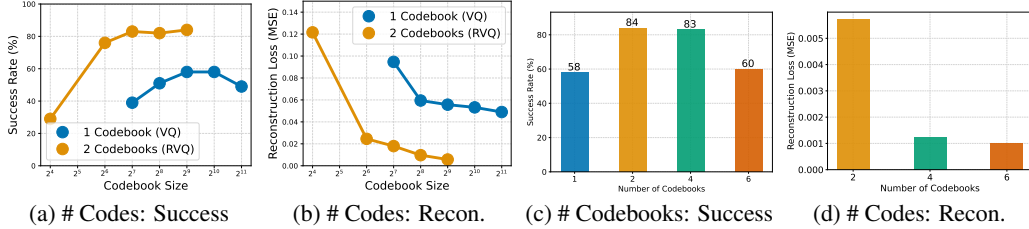


Figure 4: (a,b) show the effect of the number of codes in the codebook for RVQ and VQ on final policy success rate (see (a)) and reconstruction on unseen action trajectories in Meta-World (see (b)). (c,d) show the effect of number of codebooks on final policy success rate (see (c)) and action reconstruction (see (d)). All metrics are computed on Meta-World.

In all environments, we report the success rate as the fraction of episodes in which the agent completed the language instruction. We use the success criteria provided by each environment. We train a policy per action adapter for each environment and report the generalization performance in the main text. When reporting a single success rate per environment, it is the success averaged between all evaluation episodes containing all tasks. We give the full per-task breakdown for results in Appendix D. CALVIN, Meta-World, HabPick, and BabyAI provide expert demonstrations succeeding at the task. CALVIN has 17.9k from humans, Meta-World 22.5k from a scripted policy, HabPick 6.7k generated from an RL policy, and BabyAI 5k from a scripted policy. Full details on the train and evaluation setups per environment are in Appendix B.

We train with supervised finetuning for CALVIN, Meta-World, HabPick, and BabyAI. We train with reinforcement learning on Language Rearrangement. As described in Section 3.3 we train $\approx 140M$ parameters with LoRA [55]. We use the AdamW optimizer [59] with a learning rate of $3e^{-4}$, a warmup period of 10% of the total number of training steps, and cosine learning rate decay to 0 by the end of training. For RL, we use PPO [60]. For the learned tokenization action space adapters, we, by default, use a codebook size of 512 with 512 dimensions per codebook element. Complete hyperparameter and policy details are in Appendix C.

4.2 Continuous Action Space Adapter Comparison

We first study adapting MLLMs through Uniform, Pred, VQ, and RVQ action space adapters for the continuous action environments CALVIN, Meta-World and HabPick.

RVQ is the best performing continuous action ASA. The results in Figure 3 show that the RVQ action adapter consistently outperforms all other ASA approaches across all environments. While Pred is the second best performing method on all tasks, except on Meta-World, RVQ outperforms it by a 12% average absolute difference. One hypothesized reason for this is that Pred only learns unimodal distributions of actions, which hurts performance when learning from diverse demonstrations [43–45]. Another potential reason is the tokenization from RVQ allows the MLLM to better leverage its existing knowledge, whereas the Pred ASA requires training a new MLP network from scratch.

Uniform performs poorly on the majority of the tasks, where RVQ outperforms on average by a 27% absolute increase. A reason for this is that the Uniform discretization can fail to accurately represent the continuous actions. The performance of Uniform is also closely related to the action dimension. In Meta-World with 4 action dimensions, Uniform performs well. However, Uniform suffers with the 7 action dimensions in CALVIN and the 10 action dimensions in HabPick.

RVQ also outperforms VQ by a 18% absolute difference averaged over all environments. This is due to VQ having worse action reconstructions than RVQ. In Meta-World, both RVQ and VQ policies reach a similar cross-entropy loss on holdout trajectories during finetuning. However, on this same data, RVQ has a reconstruction mean squared error (MSE) of 0.005 while VQ has a 10x higher reconstruction MSE of 0.05. Increasing the VQ codebook size does not close this gap. We vary the VQ codebook size in powers of 2 from 2^7 to 2^{11} . Figure 4b shows the VQ reconstruction loss decreases with larger codebooks but does not even close the gap to the 2^7 RVQ codebook size. This poor reconstruction manifests in poor downstream policy performance as demonstrated by Figure 4a where policies trained with the VQ ASA plateau in success rate at codebook size 2^9 . VQ policies even decrease in performance at codebook size 2^{11} , potentially due to overfitting to the large codebook.

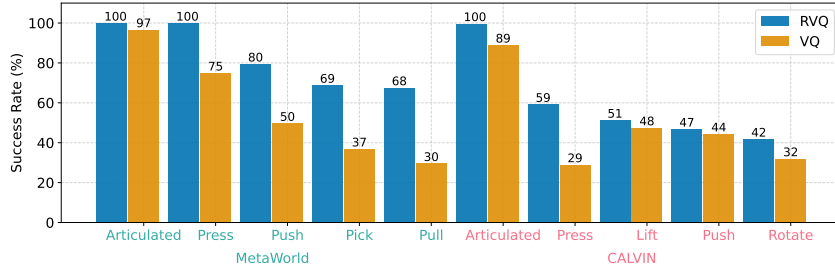


Figure 5: RVQ and VQ success per-task grouping (defined in Supp. B.6) on CALVIN and MetaWorld.

We further characterize the performance of RVQ and VQ in Figure 5 by breaking down the performance per task group in Meta-World and CALVIN. The task groups, which are fully listed in Appendix B.6, correspond to tasks with related required behaviors. Both RVQ and VQ do similarly on “articulated” object interactions (like opening drawers or doors). These tasks require less precise control since many contact points on the articulated link and broad pushing or pulling behavior can achieve the desired behavior. On the other hand, RVQ outperforms VQ on “pressing” tasks that require pushing a button. These tasks require more precise control since the agent needs to push the button all the way to a desired state. VQ often reaches the button but fails to press it all the way. The same is also true of other precise control tasks like picking, pulling, and rotating.

A potential explanation of RVQ’s success can be attributed to adaptive localization of the model’s errors, similar to prior work in residual reinforcement learning [61] and Bellman error bases [62].

A sufficient codebook size and number of codebooks are necessary for RVQ. In Figure 4a, we show that RVQ policy performance improves in performance with a larger codebook size in Meta-World. Notably, RVQ performs poorly at 29% success rate with codebook size 16 compared to 84% success at codebook size 512. These observations also align with the codebook size decreasing reconstruction error in Figure 4b. In Figure 4c, we compare the effect of the number of codebooks on performance. As earlier discussed with the performance of VQ, one codebook results in poor action reconstruction and, thus, bad policy performance. However, increasing the number of codebooks too much to 6 also hurts performance despite decreasing reconstruction loss. Likewise to the finding that Uniform performs poorly with larger action dimension since there are more tokens per action, increasing the number of codebooks also hurts policy learning.

RVQ tokens transfer to new tasks. We take the model trained on the 45 Meta-World tasks and finetune it on 5 unseen tasks. We collect 50 demonstrations for per task and finetune the policy on all task data. We use the same RVQ ASA trained only on data from the 45 tasks. Figure 6a shows the success rate of adapting RVQ compared to an Pred ASA. RVQ outperforms Pred across all tasks, achieving a 50% vs. 20% overall success rate. This demonstrates the RVQ tokens are flexible enough to be applied to new tasks.

The gains from RVQ are unique to MLLMs. Next, we analyze the unique interaction between the RVQ tokens and the MLLM policy. While we demonstrated that the RVQ ASA performs best, is this improvement due to the MLLM being able to leverage these new tokens or the added action representation ability from the separately trained RVQ decoder? To test this, we compare to two policy architectures that do not use LLMs:

- **Scratch:** This is the same architecture as the MLLM-based policy, but with a smaller 300M parameter non-pretrained transformer.
- **RT-Inspired:** This method uses a ResNet visual encoder, pretrained Flan [63] language embedding and decoder transformer-based policy. The entire policy is trained from scratch. This method is inspired by RT-1 [64], which does not have publicly released code.

Table 1 compares the effect of Pred versus RVQ ASAs on CALVIN, Meta-World and HabPick for these three policy architectures. As already established for the MLLM, RVQ is consistently better than VQ. However, for the same policy architecture trained from scratch, RVQ can hurt the performance over Pred. In CALVIN the success drops -7% and in Meta-World the performance drops -15% . This highlights that MLLM can leverage its existing knowledge about sequencing language tokens to sequencing action tokens. However, we find that for the smaller RT-Inspired policy network, the RVQ ASA consistently helps, which we hypothesize is because the added RVQ

	MLLM: Pred \rightarrow RVQ	Scratch: Pred \rightarrow RVQ	RT-Inspired: Pred \rightarrow RVQ
Calvin	68 \rightarrow 72 (+4)	50 \rightarrow 43, (-7)	35 \rightarrow 36, (+1)
Metaworld	61 \rightarrow 84 (+23)	71 \rightarrow 56, (-15)	27 \rightarrow 38, (+11)
Habitat Pick	19 \rightarrow 29 (+10)	21 \rightarrow 25, (+4)	18 \rightarrow 20, (+2)

Table 1: Comparing the effect of the RVQ action space adapter on the success rate of non-LLM based policies. Red indicates **RVQ hurts over Pred** and green indicates **RVQ helps over Pred**. RVQ typically has a negative impact on the Scratch policy, and helps the smaller RT-Inspired policy.

network and separate training help compensate for the lack of policy network capacity. We also note that RVQ may more consistently outperform Pred on demonstrations that explicitly contain multimodal action sequences [43–45].

4.3 Discrete Action Adapter Comparison

SemLang performs the best. In Figure 3, SemLang outperforms the next best ASA (Pred), by 9% on Language Rearrangement and 8% on BabyAI. SemLang performs especially well on tasks with explicit high-level language actions in Language Rearrangement (e.g., “pick apple”) where prior work has shown text-only LLM policies achieve non-zero success [21]. SemLang also does well on the BabyAI tasks with discrete low-level actions like “move left”. Additionally, Lang performs the worst in both environments, achieving 14% lower success on Language Rearrangement and 11% lower on BabyAI than SemLang. We hypothesize this is because the MLLM has to repurpose its knowledge to leverage these newly assigned action tokens, whereas a newly initialized Pred allows extracting this knowledge from the MLLM hidden state.

SemLang enables sample efficient RL. In Figure 6b, we compare the RL training curves for the ASAs in Language Rearrangement. In addition to helping with better generalization, SemLang also enables sample efficient RL training. SemLang converges in training performance after just $20M$ training samples, whereas Pred requires up to $70M$ steps to fully converge.

Token filter is crucial for language-based action spaces. In Figure 6b, we show the training of SemLang without the token filter, which restricts policy outputs to only valid action token sequences. Without the token filter, SemLang is unable to learn in the large text action space.

4.4 Empirical Comparison to Prior Work

The contributions of this work are an empirical analysis of ASAs under controlled settings on various embodied environments. Direct comparisons to prior work are challenging due to different training algorithms, policy architectures, or assumptions about input modalities. Regardless, in this section, we seek to contextualize our RVQ and SemLang MLLM results against prior work. In Meta-World,

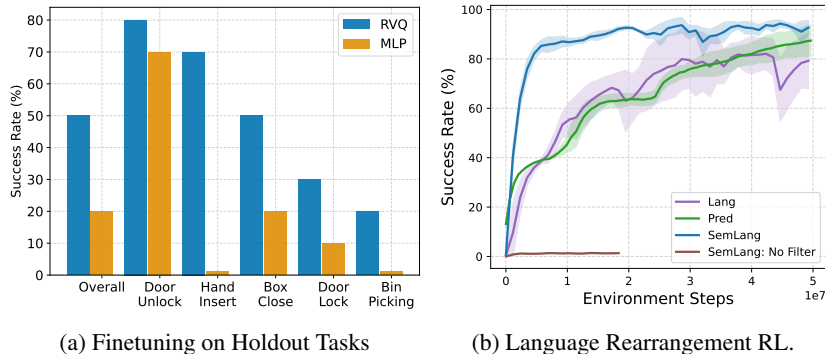


Figure 6: (a) Adapting to 5 holdout tasks from Meta-World ML-45 with 50 demos per task using the fixed RVQ tokenization. (b) RL training curves in Language Rearrangement comparing the ASAs and utility of the token filter. Displayed are averages over 2 seeds with the shaded area as the standard deviation between seeds. SemLang learns faster than other ASAs and the token filter is crucial.

to the best of our knowledge, RVQ at 84% success on ML-45 sets a new state-of-the-art result, compared to 79% from DualMind [65]. In CALVIN, RVQ at 72% success underperforms a similar work RoboFlamingo which achieves 82% success on the $ABC \rightarrow D$ split. However, RoboFlamingo uses a different MLLM and uses an additional gripper camera input. In Language Rearrangement, SemLang sets a state-of-the-art result with 51% success compared to 42% from LLaRP [21]. In BabyAI, SemLang at 40% success rate underperforms GFlan [40], which achieves 55% success. However, we use RGB visual observations, while GFlan operates from a compact, ground truth language state description. In Appendix A.1, we compare these differences in more detail.

5 Limitations and Conclusion

In this work, we studied various action space adapters (ASAs) across a variety of embodiments, action spaces, and environments. We provide a generalization of prior works through the lens of action space adapters, and for both discrete and continuous action spaces demonstrate designs that we show can leverage the knowledge within the MLLM. Our findings conclude that for continuous actions, it is best to learn action tokens that accurately model the action distribution, while for discrete actions, it is best to reason over semantic language descriptions of actions. We verify these ideas across 114 embodied AI tasks in 5 diverse environments.

A limitation of our work is all our analysis is under a single MLLM (LLaVA). Another limitation is that RVQ, the best performing ASA in continuous action spaces, requires collecting demonstrations to train the VQ model. Also, SemLang requires manually describing the actions with language. Finally, our analyses are under a single LoRA training setting. Future analyses can explore different base MLLMs under different training regimes like full LLM finetuning.

References

- [1] Jinze Bai, Shuai Bai, Shusheng Yang, Shijie Wang, Sinan Tan, Peng Wang, Junyang Lin, Chang Zhou, and Jingren Zhou. Qwen-vl: A frontier large vision-language model with versatile abilities. *arXiv preprint arXiv:2308.12966*, 2023.
- [2] Shaohan Huang, Li Dong, Wenhui Wang, Yaru Hao, Saksham Singhal, Shuming Ma, Tengchao Lv, Lei Cui, Owais Khan Mohammed, Barun Patra, Qiang Liu, Kriti Aggarwal, Zewen Chi, Johan Bjorck, Vishrav Chaudhary, Subhojit Som, Xia Song, and Furu Wei. Language is not all you need: Aligning perception with language models, 2023.
- [3] Zhiliang Peng, Wenhui Wang, Li Dong, Yaru Hao, Shaohan Huang, Shuming Ma, and Furu Wei. Kosmos-2: Grounding multimodal large language models to the world. *arXiv preprint arXiv:2306.14824*, 2023.
- [4] Junnan Li, Dongxu Li, Silvio Savarese, and Steven Hoi. Blip-2: Bootstrapping language-image pre-training with frozen image encoders and large language models, 2023.
- [5] Wenliang Dai, Junnan Li, Anthony Meng Huat Tiong, Junqi Zhao, Weisheng Wang, Boyang Li, Pascale Fung, and Steven Hoi. Instructblip: Towards general-purpose vision-language models with instruction tuning, 2023.
- [6] Haotian Liu, Chunyuan Li, Qingyang Wu, and Yong Jae Lee. Visual instruction tuning, 2023.
- [7] Chunyuan Li, Zhe Gan, Zhengyuan Yang, Jianwei Yang, Linjie Li, Lijuan Wang, and Jianfeng Gao. Multi-modal foundation models: From specialists to general-purpose assistants. *arXiv preprint arXiv:2309.10020*, 2023.
- [8] Deyao Zhu, Jun Chen, Xiaoqian Shen, Xiang Li, and Mohamed Elhoseiny. Minigpt-4: Enhancing vision-language understanding with advanced large language models. *arXiv preprint arXiv:2304.10592*, 2023.
- [9] Qinghao Ye, Haiyang Xu, Guohai Xu, Jiabo Ye, Ming Yan, Yiyang Zhou, Junyang Wang, Anwen Hu, Pengcheng Shi, Yaya Shi, et al. mplug-owl: Modularization empowers large language models with multimodality. *arXiv preprint arXiv:2304.14178*, 2023.
- [10] Bo Li, Yuanhan Zhang, Liangyu Chen, Jinghao Wang, Jingkang Yang, and Ziwei Liu. Otter: A multi-modal model with in-context instruction tuning. *arXiv preprint arXiv:2305.03726*, 2023.
- [11] Bo Li, Yuanhan Zhang, Liangyu Chen, Jinghao Wang, Fanyi Pu, Jingkang Yang, Chunyuan Li, and Ziwei Liu. Mimic-it: Multi-modal in-context instruction tuning. *arXiv preprint arXiv:2306.05425*, 2023.
- [12] Brandon McKinzie, Zhe Gan, Jean-Philippe Fauconnier, Sam Dodge, Bowen Zhang, Philipp Dufter, Dhruvi Shah, Xianzhi Du, Futang Peng, Floris Weers, et al. Mm1: Methods, analysis & insights from multimodal llm pre-training. *arXiv preprint arXiv:2403.09611*, 2024.
- [13] IDEFICS. Introducing idefics: An open reproduction of state-of-the-art visual language model. <https://huggingface.co/blog/idefics>, 2023.
- [14] Gemini Team, Rohan Anil, Sebastian Borgeaud, Yonghui Wu, Jean-Baptiste Alayrac, Jiahui Yu, Radu Soricut, Johan Schalkwyk, Andrew M Dai, Anja Hauth, et al. Gemini: a family of highly capable multimodal models. *arXiv preprint arXiv:2312.11805*, 2023.

- [15] Josh Achiam, Steven Adler, Sandhini Agarwal, Lama Ahmad, Ilge Akkaya, Florencia Leoni Aleman, Diogo Almeida, Janko Altenschmidt, Sam Altman, Shyamal Anadkat, et al. Gpt-4 technical report. *arXiv preprint arXiv:2303.08774*, 2023.
- [16] Hugo Touvron, Thibaut Lavril, Gautier Izacard, Xavier Martinet, Marie-Anne Lachaux, Timothée Lacroix, Baptiste Rozière, Naman Goyal, Eric Hambro, Faisal Azhar, et al. Llama: Open and efficient foundation language models. *arXiv preprint arXiv:2302.13971*, 2023.
- [17] Jacky Liang, Wenlong Huang, Fei Xia, Peng Xu, Karol Hausman, Brian Ichter, Pete Florence, and Andy Zeng. Code as policies: Language model programs for embodied control. *arXiv preprint arXiv:2209.07753*, 2022.
- [18] Andy Zeng, Maria Attarian, Brian Ichter, Krzysztof Choromanski, Adrian Wong, Stefan Welker, Federico Tombari, Aavek Purohit, Michael Ryoo, Vikas Sindhwani, et al. Socratic models: Composing zero-shot multimodal reasoning with language. *arXiv preprint arXiv:2204.00598*, 2022.
- [19] Anthony Brohan, Noah Brown, Justice Carbajal, Yevgen Chebotar, Xi Chen, Krzysztof Choromanski, Tianli Ding, Danny Driess, Avinava Dubey, Chelsea Finn, et al. Rt-2: Vision-language-action models transfer web knowledge to robotic control. *arXiv preprint arXiv:2307.15818*, 2023.
- [20] Xinghang Li, Minghuan Liu, Hanbo Zhang, Cunjun Yu, Jie Xu, Hongtao Wu, Chilam Cheang, Ya Jing, Weinan Zhang, Huaping Liu, et al. Vision-language foundation models as effective robot imitators. *arXiv preprint arXiv:2311.01378*, 2023.
- [21] Andrew Szot, Max Schwarzer, Harsh Agrawal, Bogdan Mazouze, Walter Talbott, Katherine Metcalf, Natalie Mackraz, Devon Hjelm, and Alexander Toshev. Large language models as generalizable policies for embodied tasks. *arXiv preprint arXiv:2310.17722*, 2023.
- [22] Stefanie Tellex, Nakul Gopalan, Hadas Kress-Gazit, and Cynthia Matuszek. Robots that use language. *Annual Review of Control, Robotics, and Autonomous Systems*, 3:25–55, 2020.
- [23] Keqin Chen, Zhao Zhang, Weili Zeng, Richong Zhang, Feng Zhu, and Rui Zhao. Shikra: Unleashing multimodal llm’s referential dialogue magic. *arXiv preprint arXiv:2306.15195*, 2023.
- [24] Haoxuan You, Haotian Zhang, Zhe Gan, Xianzhi Du, Bowen Zhang, Zirui Wang, Liangliang Cao, Shih-Fu Chang, and Yinfei Yang. Ferret: Refer and ground anything anywhere at any granularity. In *ICLR*, 2024.
- [25] Wenhai Wang, Zhe Chen, Xiaokang Chen, Jiannan Wu, Xizhou Zhu, Gang Zeng, Ping Luo, Tong Lu, Jie Zhou, Yu Qiao, et al. Visionllm: Large language model is also an open-ended decoder for vision-centric tasks. *arXiv preprint arXiv:2305.11175*, 2023.
- [26] Xin Lai, Zhuotao Tian, Yukang Chen, Yanwei Li, Yuhui Yuan, Shu Liu, and Jiaya Jia. Lisa: Reasoning segmentation via large language model. *arXiv preprint arXiv:2308.00692*, 2023.
- [27] Hao Zhang, Hongyang Li, Feng Li, Tianhe Ren, Xueyan Zou, Shilong Liu, Shijia Huang, Jianfeng Gao, Lei Zhang, Chunyuan Li, et al. Llava-grounding: Grounded visual chat with large multimodal models. *arXiv preprint arXiv:2312.02949*, 2023.
- [28] Michael Ahn, Anthony Brohan, Noah Brown, Yevgen Chebotar, Omar Cortes, Byron David, Chelsea Finn, Chuyuan Fu, Keerthana Gopalakrishnan, Karol Hausman, et al. Do as i can, not as i say: Grounding language in robotic affordances. *arXiv preprint arXiv:2204.01691*, 2022.
- [29] Danny Driess, Fei Xia, Mehdi SM Sajjadi, Corey Lynch, Aakanksha Chowdhery, Brian Ichter, Ayzaan Wahid, Jonathan Tompson, Quan Vuong, Tianhe Yu, et al. PaLM-E: An embodied multimodal language model. *arXiv preprint arXiv:2303.03378*, 2023.
- [30] Oier Mees, Lukas Hermann, Erick Rosete-Beas, and Wolfram Burgard. Calvin: A benchmark for language-conditioned policy learning for long-horizon robot manipulation tasks. *IEEE Robotics and Automation Letters*, 7(3):7327–7334, 2022.
- [31] Tianhe Yu, Deirdre Quillen, Zhanpeng He, Ryan Julian, Karol Hausman, Chelsea Finn, and Sergey Levine. Meta-world: A benchmark and evaluation for multi-task and meta reinforcement learning. In *Conference on robot learning*, pages 1094–1100. PMLR, 2020.
- [32] Dhruv Shah, Błażej Osiański, Sergey Levine, et al. Lm-nav: Robotic navigation with large pre-trained models of language, vision, and action. In *Conference on Robot Learning*, pages 492–504. PMLR, 2023.
- [33] Wenlong Huang, Fei Xia, Ted Xiao, Harris Chan, Jacky Liang, Pete Florence, Andy Zeng, Jonathan Tompson, Igor Mordatch, Yevgen Chebotar, et al. Inner monologue: Embodied reasoning through planning with language models. *arXiv preprint arXiv:2207.05608*, 2022.
- [34] Jacky Liang, Wenlong Huang, Fei Xia, Peng Xu, Karol Hausman, Brian Ichter, Pete Florence, and Andy Zeng. Code as policies: Language model programs for embodied control. In *2023 IEEE International Conference on Robotics and Automation (ICRA)*, pages 9493–9500. IEEE, 2023.
- [35] Wenlong Huang, Fei Xia, Dhruv Shah, Danny Driess, Andy Zeng, Yao Lu, Pete Florence, Igor Mordatch, Sergey Levine, Karol Hausman, et al. Grounded decoding: Guiding text generation with grounded models for robot control. *arXiv preprint arXiv:2303.00855*, 2023.
- [36] Jimmy Wu, Rika Antonova, Adam Kan, Marion Lepert, Andy Zeng, Shuran Song, Jeannette Bohg, Szymon Rusinkiewicz, and Thomas Funkhouser. Tidybot: Personalized robot assistance with large language models. *arXiv preprint arXiv:2305.05658*, 2023.
- [37] Tom Silver, Soham Dan, Kavitha Srinivas, Joshua B Tenenbaum, Leslie Pack Kaelbling, and Michael Katz. Generalized planning in pddl domains with pretrained large language models. *arXiv preprint arXiv:2305.11014*, 2023.

- [38] Guanzhi Wang, Yuqi Xie, Yunfan Jiang, Ajay Mandlekar, Chaowei Xiao, Yuke Zhu, Linxi Fan, and Anima Anandkumar. Voyager: An open-ended embodied agent with large language models. *arXiv preprint arXiv:2305.16291*, 2023.
- [39] Ruizhe Shi, Yuyao Liu, Yanjie Ze, Simon S Du, and Huazhe Xu. Unleashing the power of pre-trained language models for offline reinforcement learning. *arXiv preprint arXiv:2310.20587*, 2023.
- [40] Thomas Carta, Clément Romac, Thomas Wolf, Sylvain Lamprier, Olivier Sigaud, and Pierre-Yves Oudeyer. Grounding large language models in interactive environments with online reinforcement learning. *arXiv preprint arXiv:2302.02662*, 2023.
- [41] Ayush Jain, Andrew Szot, and Joseph J Lim. Generalization to new actions in reinforcement learning. *arXiv preprint arXiv:2011.01928*, 2020.
- [42] Gabriel Dulac-Arnold, Richard Evans, Hado van Hasselt, Peter Sunehag, Timothy Lillicrap, Jonathan Hunt, Timothy Mann, Theophane Weber, Thomas Degris, and Ben Coppin. Deep reinforcement learning in large discrete action spaces. *arXiv preprint arXiv:1512.07679*, 2015.
- [43] Nur Muhammad Shafiullah, Zichen Cui, Ariuntuya Arty Altanzaya, and Lerrel Pinto. Behavior transformers: Cloning k modes with one stone. *Advances in neural information processing systems*, 35:22955–22968, 2022.
- [44] Zichen Jeff Cui, Yibin Wang, Nur Muhammad Mahi Shafiullah, and Lerrel Pinto. From play to policy: Conditional behavior generation from uncurated robot data. *arXiv preprint arXiv:2210.10047*, 2022.
- [45] Seungjae Lee, Yibin Wang, Haritheja Etukuru, H Jin Kim, Nur Muhammad Mahi Shafiullah, and Lerrel Pinto. Behavior generation with latent actions. *arXiv preprint arXiv:2403.03181*, 2024.
- [46] Zhiliang Peng, Wenhui Wang, Li Dong, Yaru Hao, Shaohan Huang, Shuming Ma, and Furu Wei. Kosmos-2: Grounding multimodal large language models to the world. *arXiv preprint arXiv:2306.14824*, 2023.
- [47] Qian Sun, Yufeng Cui, Xiaosong Zhang, Fan Zhang, Qiying Yu, Zhengxiong Luo, Yuezhe Wang, Yongming Rao, Jingjing Liu, Tiejun Huang, et al. Generative multimodal models are in-context learners. *arXiv preprint arXiv:2312.13286*, 2023.
- [48] Tianhe Yu, Ted Xiao, Austin Stone, Jonathan Tompson, Anthony Brohan, Su Wang, Jaspier Singh, Clayton Tan, Jodilyn Peralta, Brian Ichter, et al. Scaling robot learning with semantically imagined experience. *arXiv preprint arXiv:2302.11550*, 2023.
- [49] Emanuele Aiello, Lili Yu, Yixin Nie, Armen Aghajanyan, and Barlas Oguz. Jointly training large autoregressive multimodal models. *arXiv preprint arXiv:2309.15564*, 2023.
- [50] Doyup Lee, Chiheon Kim, Saehoon Kim, Minsu Cho, and Wook-Shin Han. Autoregressive image generation using residual quantization. In *Proceedings of the IEEE/CVF Conference on Computer Vision and Pattern Recognition*, pages 11523–11532, 2022.
- [51] Neil Zeghidour, Alejandro Luebs, Ahmed Omran, Jan Skoglund, and Marco Tagliasacchi. Soundstream: An end-to-end neural audio codec. *IEEE/ACM Transactions on Audio, Speech, and Language Processing*, 30:495–507, 2021.
- [52] Richard Bellman. A markovian decision process. *Indiana Univ. Math. J.*, 6:679–684, 1957. ISSN 0022-2518.
- [53] Andrew Jaegle, Sebastian Borgeaud, Jean-Baptiste Alayrac, Carl Doersch, Catalin Ionescu, David Ding, Skanda Koppula, Daniel Zoran, Andrew Brock, Evan Shelhamer, et al. Perceiver io: A general architecture for structured inputs & outputs. *arXiv preprint arXiv:2107.14795*, 2021.
- [54] Aaron Van Den Oord, Oriol Vinyals, et al. Neural discrete representation learning. *Advances in neural information processing systems*, 30, 2017.
- [55] Edward J Hu, Yelong Shen, Phillip Wallis, Zeyuan Allen-Zhu, Yuanzhi Li, Shean Wang, Lu Wang, and Weizhu Chen. Lora: Low-rank adaptation of large language models. *arXiv preprint arXiv:2106.09685*, 2021.
- [56] Tianhe Yu, Deirdre Quillen, Zhanpeng He, R. Julian, Karol Hausman, Chelsea Finn, and S. Levine. Meta-world: A benchmark and evaluation for multi-task and meta reinforcement learning. In *CoRL*, 2019.
- [57] Andrew Szot, Alexander Clegg, Eric Undersander, Erik Wijmans, Yili Zhao, John Turner, Noah Maestre, Mustafa Mukadam, Devendra Singh Chaplot, Oleksandr Maksymets, et al. Habitat 2.0: Training home assistants to rearrange their habitat. *Advances in Neural Information Processing Systems*, 34, 2021.
- [58] Maxime Chevalier-Boisvert, Dzmitry Bahdanau, Salem Lahlou, Lucas Willems, Chitwan Saharia, Thien Huu Nguyen, and Yoshua Bengio. BabyAI: First steps towards grounded language learning with a human in the loop. In *ICLR*, 2019. URL <https://openreview.net/forum?id=rJeXCo0cYX>.
- [59] Ilya Loshchilov and Frank Hutter. Decoupled weight decay regularization. *arXiv preprint arXiv:1711.05101*, 2017.
- [60] John Schulman, Filip Wolski, Prafulla Dhariwal, Alec Radford, and Oleg Klimov. Proximal policy optimization algorithms. *arXiv preprint arXiv:1707.06347*, 2017.
- [61] Tobias Johannink, Shikhar Bahl, Ashvin Nair, Jianlan Luo, Avinash Kumar, Matthias Loskyll, Juan Aparicio Ojea, Eugen Solowjow, and Sergey Levine. Residual reinforcement learning for robot control. In *2019 international conference on robotics and automation (ICRA)*, pages 6023–6029. IEEE, 2019.
- [62] Ronald Parr, Lihong Li, Gavin Taylor, Christopher Painter-Wakefield, and Michael L Littman. An analysis of linear models, linear value-function approximation, and feature selection for reinforcement learning. In *Proceedings of the 25th international conference on Machine learning*, pages 752–759, 2008.

- [63] Jason Wei, Maarten Bosma, Vincent Y Zhao, Kelvin Guu, Adams Wei Yu, Brian Lester, Nan Du, Andrew M Dai, and Quoc V Le. Finetuned language models are zero-shot learners. *arXiv preprint arXiv:2109.01652*, 2021.
- [64] Anthony Brohan, Noah Brown, Justice Carbajal, Yevgen Chebotar, Joseph Dabis, Chelsea Finn, Keerthana Gopalakrishnan, Karol Hausman, Alex Herzog, Jasmine Hsu, et al. Rt-1: Robotics transformer for real-world control at scale. *arXiv preprint arXiv:2212.06817*, 2022.
- [65] Yao Wei, Yanchao Sun, Ruijie Zheng, Sai Vemprala, Rogerio Bonatti, Shuhang Chen, Ratnesh Madaan, Zhongjie Ba, Ashish Kapoor, and Shuang Ma. Is imitation all you need? generalized decision-making with dual-phase training. In *Proceedings of the IEEE/CVF International Conference on Computer Vision*, pages 16221–16231, 2023.
- [66] Ankesh Anand, Jacob Walker, Yazhe Li, Eszter Vértés, Julian Schrittwieser, Sherjil Ozair, Théophane Weber, and Jessica B Hamrick. Procedural generalization by planning with self-supervised world models. *arXiv preprint arXiv:2111.01587*, 2021.
- [67] Julian Schrittwieser, Ioannis Antonoglou, Thomas Hubert, Karen Simonyan, Laurent Sifre, Simon Schmitt, Arthur Guez, Edward Lockhart, Demis Hassabis, Thore Graepel, et al. Mastering atari, go, chess and shogi by planning with a learned model. *Nature*, 588(7839):604–609, 2020.
- [68] Scott Reed, Konrad Zolna, Emilio Parisotto, Sergio Gomez Colmenarejo, Alexander Novikov, Gabriel Barth-Maron, Mai Gimenez, Yury Sulsky, Jackie Kay, Jost Tobias Springenberg, et al. A generalist agent. *arXiv preprint arXiv:2205.06175*, 2022.
- [69] Tsung-Wei Ke, Nikolaos Gkanatsios, and Katerina Fragkiadaki. 3d diffuser actor: Policy diffusion with 3d scene representations. *arXiv preprint arXiv:2402.10885*, 2024.
- [70] Andrew Szot, Karmesh Yadav, Alex Clegg, Vincent-Pierre Berges, Aaron Gokaslan, Angel Chang, Manolis Savva, Zsolt Kira, and Dhruv Batra. Habitat rearrangement challenge 2022. https://aihabitat.org/challenge/2022_rearrange, 2022.
- [71] Thomas Wolf, Lysandre Debut, Victor Sanh, Julien Chaumond, Clement Delangue, Anthony Moi, Pierric Cistac, Tim Rault, Rémi Louf, Morgan Funtowicz, et al. Huggingface’s transformers: State-of-the-art natural language processing. *arXiv preprint arXiv:1910.03771*, 2019.
- [72] Adam Paszke, Sam Gross, Francisco Massa, Adam Lerer, James Bradbury, Gregory Chanan, Trevor Killeen, Zeming Lin, Natalia Gimelshein, Luca Antiga, et al. Pytorch: An imperative style, high-performance deep learning library. *Advances in neural information processing systems*, 32, 2019.
- [73] Jeff Rasley, Samyam Rajbhandari, Olatunji Ruwase, and Yuxiong He. Deepspeed: System optimizations enable training deep learning models with over 100 billion parameters. In *Proceedings of the 26th ACM SIGKDD International Conference on Knowledge Discovery & Data Mining*, pages 3505–3506, 2020.

Work	Environments	Best ASA	Other ASAs Studied	Action Space Types	Training	Using LLM/VLM?
RoboFlamingo [20]	CALVIN	MLP	-	Continuous	BC	✓
Lamo [39]	Franka Kitchen, Atari, MuJoCo	MLP	-	Continuous, Discrete	Offline-RL	✓
GFlan [40]	BabyAI	Sem Lang (scoring)	-	Discrete	Online-RL	✓
RT-2 [19]	Internal	Uniform	-	Continuous	BC	✓
LLaRP [21]	Language Rearrangement	MLP	-	Discrete	Online-RL	✓
VQ-BcT [45]	PushT, Multimodal Ant, BlockPush, Franka Kitchen, nuScenes, PlayKitchen	RVQ+MLP	-	Continuous	BC	✗
Ours	Language Rearrangement, Baby AI, Meta-World, CALVIN, Habitat Skills	RVQ/ Sem-Lang	MLP, VQ, Uniform, Non-Sem, Non-Sem Comp	Continuous, Discrete	Online-RL, BC	✓

Table 2: Comparing our investigation to prior work. Prior work typically analyzes a single action adapter in a single environment. We study a variety of action adapters across a variety of environments.

A Prior Work Comparison

In this section we expand on the differences between the prior work in action space adaptation mentioned in Section 2 and our investigation. Table 2 compares our investigation to prior work along several key dimensions. We emphasize that unlike prior works, ours studies a variety of action space adapters under a greater diversity of environments.

A.1 Empirical Comparison to Prior Work

We report performance on standard benchmarks which prior work has also extensively studied. However, even within the benchmarks there are differences in training algorithms and sensor input assumptions that make direct comparison to prior work difficult. Regardless of these differences, we study different ASAs for MLLMs in a consistent experimental setting. We also describe differences between the empirical setups of ours and prior works that perform well on these benchmarks.

Meta-World (MLLM +RVQ 84% success rate on ML-45): To the best of our knowledge, our 84% is the highest reported on Meta-World ML-45 so far. Anand et al. [66] operates under similar sensor assumptions and achieves 77% success with MuZero [67]. DualMind [65] achieves 79% success rate on ML-45 and outperforms other generalist agents like Gato [68]. However, DualMind uses privileged simulator information about the joint states and object positions while we only use RGB visual observations.

CALVIN (MLLM +RVQ 72% success rate): RoboFlamingo achieves a higher 82% success rate on the same $ABC \rightarrow D$ task. However, RoboFlamingo uses the OpenFlamingo VLM while we use LLaVA. RoboFlamingo use the gripper and fixed camera while we only use the fixed camera. More recent work like 3D Diffuser Actor [69] practically solves the $ABC \rightarrow D$ task, achieving 96% success rate. However, this work uses depth inputs, and a diffusion model policy that predicts keypoints for the end-effector rather than underlying actions. Our work uses only RGB visuals, uses a MLLM policy and predicts relative end-effector poses rather than keypoints.

Language Rearrangement (SemLang 51% success rate): This outperforms the prior highest reported number of 42% on the overall evaluation set from LLaRP [21].

BabyAI (SemLang 40% success rate): GFlan [40] achieves 55% success on the same evaluation split. However, the GFlan policy takes as input a ground truth language description of the state, while our policies take as input a 200×200 RGB top down rendering of the environment. GFlan also trains the policy with reinforcement learning while we train with supervised learning.

B Environment Details

An overview of the environments is visualized in Figure 7. This figure visualizes the training observations input to the agent. We run experiments on 5 environments, and each environment in turn consists of multiple tasks. We arrive at the task count of 114 in the main paper through 45 tasks in Meta-World, 34 in CALVIN, 20 in HabPick where we count each object goal as a different task, 10 in Language Rearrangement for each of the evaluation splits, and 5 in BabyAI. The task count for Language Rearrangement is conservative since technically it consists of 282 instruction templates, each of which corresponds to a distinct task and goal.

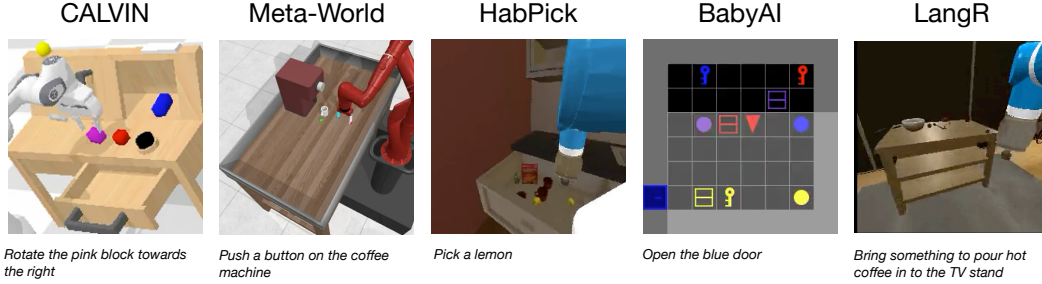


Figure 7: Visualizations of the environments we study. The top row shows an observation in the environment. The bottom row shows the associated instruction in that episode.

B.1 Meta-World

Tasks: We use the ML-45 benchmark from Meta-World [56]. Each of the 45 tasks are specified with a fixed language instruction. We use the task descriptions from Appendix Section A of Yu et al. [56].

Observation Space: 200×200 RGB images from a fixed camera position. To render the visual observations, we only use the “corner4” camera position as this gives an unobstructed view of the robot in most of the tasks.

Action Space: 4DoF continuous control of the arm and gripper. The first 3 dimensions specify the relative end-effector translation. The last dimension specifies the desired gripper state.

Training: We use 40 start and goal configurations for each of the tasks. We generate 500 demonstrations for each of the 45 tasks. We use the scripted policies from Yu et al. [56]. At each step we add Gaussian noise $\mathcal{N}(0, 0.1)$ to the actions produced by the scripted policy before executing it in the environment. We generate 500 successful trajectories per task, resulting in $45 \cdot 500 = 22.5k$ total trajectories.

Evaluation: We evaluate performance on 10 unseen start and goal configurations for each of the 45 tasks. So in total, we evaluate on 450 unseen configurations and report the average performance over these 450 episodes.

B.2 CALVIN

Tasks: We use the CALVIN $ABC \rightarrow D$ dataset split.

Observation Space: 200×200 RGB observations from the fixed camera view.

Action Space: 7DoF continuous control of the arm and gripper. The first 6 dimensions specify the relative position and rotation of the end-effector. The final dimension is a binary indicator for if the gripper should be open or closed. We hold out 1024 subsequences of the policy context length from these trajectories for reporting validation performance during the SFT process.

Training: We use the 17,871 demonstrations provided in the CALVIN $ABC \rightarrow D$ dataset. These demonstrations are in 3 different table backgrounds. This also includes 1,088 demonstrations for validation.

Evaluation: We report performance on the D split. This evaluation scene is a different color than that encountered during training. All the start positions and goals are also different. Many of the language instructions are also unseen from training. We report the average performance over the 1,000 evaluation sequences. We report the success of the first task completed in the sequence.

B.3 Habitat Pick

Tasks: We use the same Pick task as in Habitat 2.0 Geometric Goal object rearrangement [57, 70], except we provide the agent the name of the object to rearrange rather than the starting coordinates of the object and increase the observation resolution. The task is successful when the agent picks up the object and returns the end-effector within a fixed offset to a “resting position” in front of the robot.

The task ends in failure if the agent excessively collides with the scene, drops the object, or picks up the wrong object. The agent starts within 2 meters of the object and facing towards the receptacle but with random noise $\mathcal{N}(0, 1.57)$ applied to the direction of facing directly at the receptacle. The maximum number of steps per episode is 300 steps.

Observation Space: A 336×336 head-mounted RGB camera.

Action Space: The action space is 10DoF control of the arm, base and gripper. The first 2 dimensions control the linear and angular velocity of the base. The next 7 dimensions control the relative joint offsets of the arm. The final dimension controls whether the suction gripper is engaged or not.

Training: We first train a privileged policy with RL to complete the task. This policy takes as input the egocentric depth image and the ground truth position of the target object to pick up. We collect $20k$ successful trajectories.

Evaluation: We evaluate on the test episodes from Szot et al. [70] which are 1,000 episodes in unseen home layouts.

B.4 BabyAI

Tasks: The tasks all occur in a 6×6 grid populated with interactable objects. We use the task definitions from Carta et al. [40]. This consists of the following 5 instruction templates: “Go to <object>”, “Pick up <object>”, “Put <object A> next to <object B>”, “Pick up <object A> then go to <object B> and Go to <object B> after pick up <object A>”, “Unlock <door>”. The maximum number of steps per episode is 50 steps.

Observation Space: 200×200 RGB observation as a top down of the 6×6 scene. Note this is a more challenging observation space than prior gridworld navigation tasks that provide the current view as a compact entity specific array [58] or by a language description [40].

Action Space: The action space consists of 6 actions consisting of: turn left, turn right, move forward, pick, drop and toggle.

Training: We collect 1,000 demonstrations for each of the 5 templates. We randomly sample an instruction and starting state configuration for every demonstration. We use the expert planner from Chevalier-Boisvert et al. [58] to generate the demonstrations.

Evaluation: We report performance on the unseen synonyms generalization test, described in Section 4.2 of Carta et al. [40]. We evaluate on 20 episodes per template type, giving 100 total evaluation episodes.

B.5 Language Rearrangement

Tasks: An agent starts in an unseen house and must complete a rearrangement task from a language instruction.

Observation Space: The agent has a 336×336 head-mounted RGB camera. We increase the camera resolution from 256×256 in the original Language Rearrangement task to match the input resolution of the LLaVA CLIP encoder.

Action Space: We use the same action space as from the original Language Rearrangement benchmark Szot et al. [21]. The agent can select between 70 high-level skills that include picking up objects by name, navigating to receptacles, placing on receptacles by name, and opening and closing receptacles by name.

Training: Since Language Rearrangement does not provide any demonstrations and due to the emphasis on exploration in the problem, they are not readily obtainable, even with oracle planners. Therefore, we opt to train policies with reinforcement learning from the environment reward provided by the Language Rearrangement task.

Evaluation: We evaluate on all 10 evaluation datasets from Language Rearrangement consisting of 1,000 evaluation episodes on unseen scenes.

B.6 Task Groupings

In Section 4 we breakdown the performance on CALVIN and MetaWorld for task groupings. Each of the task groupings consists of multiple tasks from the benchmark. We grouped tasks in the following way:

MetaWorld:

- Articulated: “door-close”, “door-open”, “drawer-close”, “drawer-open”, “faucet-open”, “faucet-close”, “handle-press-side”, “handle-press”, “window-open”, “window-close”
- Press: “button-press-topdown”, “button-press-topdown-wall”, “button-press”, “button-press-wall”, “coffee-button”
- Push: “plate-slide”, “plate-slide-side”, “plate-slide-back”, “plate-slide-back-side”, “push-back”, “push”, “push-wall”, “stick-push”, “sweep-into”, “sweep”, “soccer”, “coffee-push”
- Pick: “assembly”, “basketball”, “dial-turn”, “disassemble”, “hammer”, “peg-insert-side”, “peg-unplug-side”, “pick-out-of-hole”, “pick-place”, “pick-place-wall”, “reach”, “reach-wall”, “shelf-place”
- Pull: “coffee-pull”, “handle-pull-side”, “handle-pull”, “lever-pull”, “stick-pull”

CALVIN:

- Articulated: “move slider left”, “open drawer”, “close drawer”, “move slider right”
- Press: “turn off led”, “turn on led”, “turn on lightbulb”, “turn off lightbulb”
- Lift: “lift blue block slider”, “lift pink block table”, “lift red block slider”, “lift red block table”, “lift pink block slider”, “lift blue block table”
- Push: “push pink block right”, “push blue block right”, “push red block left”, “push pink block left”, “push red block right”, “push blue block left”, “push into drawer”
- Rotate: “rotate red block right”, “rotate red block left”, “rotate pink block left”, “rotate pink block right”, “rotate blue block right”, “rotate blue block left”

C Further Policy Details

C.1 Prompt Details

In addition to inputting the task instruction to the LLM, we also format the instruction with a prompt. We base our prompt off the prompt used in LLaVA. For all continuous control tasks, we use the prompt template “Prompt: control the robot. USER: <INSTRUCTION> ASSISTANT: ”. For discrete action space tasks, we describe the available actions to the agent in the prompt as well. For BabyAI, this is the prompt template “Prompt: Control the red triangle to complete the instruction using left, right, forward, pick, drop and toggle. USER: <INSTRUCTION> ASSISTANT: ”. For Language Rearrangement, this is the prompt template “Prompt: You are a home robot assistant. Your possible actions are: pick object, place receptacle, nav receptacle, open receptacle, close receptacle, STOP. - Objects: ball, clamp, hammer, screwdriver, padlock, scissors, block, drill, spatula, knife, spoon, plate, sponge, cleanser, plum, pear, peach, apple, lemon, can, box, banana, strawberry, lego, cube, book, bowl, cup, mug, orange, lid, toy, wrench. - Receptacles: chair, black table, brown table, TV stand, sink, right counter, left counter, sofa, fridge, left drawer, right drawer, middle drawer. USER: <INSTRUCTION> ASSISTANT: ”.

C.2 Action Space Adapter Details

We use the same ASA details between all environments. We detail the architecture and training decisions for the different ASAs when applicable.

VQ: Use a codebook size of 512 with 512 dimensions per codebook element. These 512 tokens are mapped to token indices 31000 – 31512 from the LLaMA language modeling head. The encoder and decoder networks for predicting the latent and decoding from the latent are 4 layer MLP networks with hidden size 2048 using ReLU activations. The VQ network is trained on the actions in the same dataset used to train the policy. The network is trained with MSE loss to reconstruct the original actions. We VQ network for 3 epochs over the dataset.

RVQ: Use all the same details as VQ, but with a Residual-VQ that uses 2 codebooks.

Hyperparameter	CALVIN	Meta-World	BabyAI	HabPick
LR	$3e^{-4}$	$3e^{-4}$	$3e^{-4}$	$3e^{-4}$
Optimizer	AdamW	AdamW	AdamW	AdamW
Number of Epochs	3	3	20	20
Batch Size Per GPU	32	32	8	32
Context Length	12	3	32	3
Max Gradient Norm	1	1	1	1

Table 3: Hyperparameters for all imitation learning experiments. Most hyperparameters are the same between environments but the number of training epochs, context length and batch size per GPU are adjusted to fit the need for history, environment dataset size and task complexity.

Pred: We use a 2 layer MLP network with a hidden size of 2048 and ReLU activations. We use this same MLP network architecture for discrete and continuous action space tasks. In the robot manipulation tasks, we also found it useful to include the robot proprioception as input to the MLP network and included this as input to the network layer. The robot proprioception consists of the robot joint angles and the gripper state. This ASA requires no separate training.

Uniform: In the tasks we consider, the actions are already normalized to be in $[-1, 1]$. We then create 512 evenly spaced bins within this interval and assign each action dimension based on which bin it is within. Like with VQ, we assign the 512 tokens to indices 31000 – 31512 from the LLaMA language modeling head. This ASA requires no separate training.

Lang: Starting from the same semantic tokenization as with SemLang, we remap each token to the token corresponding to a digit “0” to “9”. Therefore, the token count per action is the same between Lang and SemLang, but the Lang action tokens have no semantic meaning being just digits.

C.3 Training and Architecture Details

We use all pretrained components from LLaVA. For the visual token downsampler, we use a 2 layer Perceiver network [53] with 4 output latents and hidden size 4096.

We detail the hyperparameters used for imitation learning in in Table 3. We trained with the HuggingFace Transformers library [71], PyTorch [72], DeepSpeed [73]. For reinforcement learning, we use learning rate $3e^{-4}$, 32 steps per rollout. 18 parallel environment workers per GPU, an entropy coefficient of 0.01, 2 epochs over the data batch per rollout, 6 PPO minibatches, a maximum gradient norm of 0.2 and $\gamma = 0.99$.

We train the CALVIN, Meta-World and HabPick imitation learning results on a 4xA40 GPU setup. We train the Language Rearrangement and BabyAI experiments on a 8xA100-80GB GPU setup.

We train the LLM weights with LoRA and fine tune the entire ASA and downsampler module. For LoRA we use rank value 128, alpha parameter 32 and dropout 0.1.

D Per-Task Breakdown

In this section, we show results for each environment by task type. Table 4 shows performance on Language Rearrangement for each of the evaluation datasets. Table 5 shows performance on CALVIN for each of the CALVIN tasks. Table 6 shows performance on BabyAI for each of the BabyAI instruction types. Table 7 shows performance on Meta-World for each of the 45 Meta-World task types.

	Total	Aggregated			Per Dataset Breakdown										
		Behavior Generalization	Paraphrastic Robustness		Train	Scene	Instruct Rephrasing	Novel Objects	Multiple Rearrange	Referring Expressions	Context	Irrelevant Text	Multiple Objects	Spatial	Conditional Instructs
SemLang	51 ± 1	56 ± 2	47 ± 1		94 ± 3	94 ± 6	92 ± 1	97 ± 0	80 ± 6	31 ± 3	46 ± 14	66 ± 6	2 ± 2	0 ± 0	46 ± 4
Lang	27 ± 12	31 ± 14	24 ± 10		72 ± 13	58 ± 11	74 ± 12	76 ± 29	21 ± 10	10 ± 12	12 ± 11	20 ± 13	0 ± 0	2 ± 3	26 ± 16
Pred	42 ± 2	45 ± 3	38 ± 1		99 ± 1	96 ± 4	92 ± 2	95 ± 4	47 ± 5	26 ± 2	34 ± 2	32 ± 2	0 ± 1	8 ± 1	39 ± 3

Table 4: Evaluation results at 20M steps of RL training for all results in Language Rearrangement. We show averages and standard deviations over 2 random seeds of full policy training.

	RVQ	Pred	VQ	Uniform
CALVIN	72	68	56	28
turn off led	50	96	36	16
move slider left	99	100	100	15
rotate red block right	54	17	35	17
open drawer	100	100	56	100
rotate red block left	31	14	14	14
push pink block right	31	100	51	14
push blue block right	42	27	35	20
push red block left	68	36	61	17
push pink block left	47	50	86	14
push red block right	35	35	17	17
push blue block left	56	27	47	14
push into drawer	49	34	14	14
rotate pink block left	76	73	73	16
turn on lightbulb	80	34	19	9
rotate pink block right	30	73	19	10
rotate blue block right	28	13	13	13
turn off lightbulb	76	19	19	12
lift blue block table	34	25	34	16
close drawer	100	100	100	70
rotate blue block left	32	11	38	20
move slider right	100	100	100	19
turn on led	31	100	42	14
lift blue block slider	32	22	51	15
lift pink block table	66	68	82	11
lift red block slider	56	22	41	13
lift red block table	45	53	15	15
lift pink block slider	75	12	62	12

Table 5: Breakdown on every CALVIN task. Note there are not an equal proportion of all tasks in the evaluation dataset.

	SemLang	Lang	Pred
goto	90	90	75
pickup	60	35	35
open	26	6	21
putnext	7	7	7
pick up seq go to	20	10	25

Table 6: Breakdown on every BabyAI task.

	RVQ	Pred	VQ	Uniform
Meta-World	84	61	58	75
assembly	95	70	5	60
basketball	85	70	55	100
button-press-topdown	100	90	36	100
button-press-topdown-wall	100	100	57	90
button-press	100	100	85	100
button-press-wall	100	100	100	100
coffee-button	100	100	97	100
coffee-pull	96	40	26	50
coffee-push	75	20	25	80
dial-turn	96	50	36	100
disassemble	55	30	25	50
door-close	100	100	100	100
door-open	100	100	100	100
drawer-close	100	100	100	100
drawer-open	100	100	73	100
faucet-open	100	100	100	100
faucet-close	100	90	100	60
hammer	100	40	45	20
handle-press-side	100	100	100	100
handle-press	100	100	94	100
handle-pull-side	36	10	6	10
handle-pull	65	20	45	30
lever-pull	55	40	45	40
peg-insert-side	64	70	4	40
peg-unplug-side	54	30	94	90
pick-out-of-hole	45	90	35	30
pick-place	74	20	44	60
pick-place-wall	75	20	35	30
plate-slide	100	60	44	100
plate-slide-side	100	100	100	90
plate-slide-back	100	90	14	100
plate-slide-back-side	100	20	100	100
push-back	45	30	15	20
push	64	20	74	90
push-wall	76	40	56	100
reach	34	20	14	70
reach-wall	75	80	75	70
shelf-place	43	20	13	10
soccer	44	0	64	40
stick-push	100	60	5	100
stick-pull	86	50	26	100
sweep-into	65	40	55	70
sweep	85	30	45	70
window-open	100	100	100	100
window-close	100	100	100	100

Table 7: Breakdown on every Meta-World task.